



Heat Transfer Performance of Latent Heat Storage Medium Infiltrated in Porous Aluminium- Experimental Approach

Njoku Romanus Egwuonwu

^oDepartment of Metallurgical and Materials Engineering, University of Nigeria, Nsukka

*Corresponding author E-mail address: romanus.njoku@unn.edu.ng

ISSN: 2582-3353



Publication details

Received: 30th August 2020
Revised: 28th September 2020
Accepted: 28th September 2020
Published: 27th October 2020

Abstract: Thermal energy storage unit with phase change material (PCM) is a critical component of many solar heating/solar power plants and waste heat recovery systems. However, the intrinsically low thermal conductivity of PCMs is their major drawback leading to the inefficiency of these thermal energy storage systems. An experimental set-up was designed to evaluate the transient thermal behaviour of phase change material (PCM)/porous aluminium composites. Stearic acid wax was used as PCM and was infiltrated into porous aluminium structures to enhance effective thermal conductivity and thermal diffusivity. Porous aluminium structures were manufactured by infiltrating liquid aluminium through the inter-granular pore spaces created inside a sodium chloride bead pack. Samples were characterized using scanning electron microscopy and optical microscopy. A test rig was developed that consisted of a heat source, K-type thermocouples, infrared camera, data logging instruments and computers equipped with "Altair" software. The result indicated that the system parameters of the PCM/porous aluminium composite have a significant effect in its heat transfer behaviour. The heat transfer performance of the PCM/porous aluminium composite was increased significantly (up to 8- 13 times depending on the morphology of the porous structure) relative to the pure stearic acid PCM. The rate of change of temperature within the composites was found to be dependent upon the balance between the relative density and window diameter of the porous aluminium structures.

Keywords: PCM; stearic acid; porous aluminium; heat transfer performance; relative density; window size

1. Introduction

With global concern over depletion of fossil fuels and the environmental pollution associated with their use, clean renewable energy such as solar energy is gaining attention nowadays. In addition, significant amount of waste heat in industries is discharged into the environment without recovery, causing serious energy waste problems. Incidentally, most of such energy sources (solar and waste heat) are characterized by intermittence and instability which may result in the imbalance between energy supply and energy consumption. The thermal energy storage technology is a promising approach to deal with these challenges by providing efficient energy saving which bridges the gap between energy supply and demand and improves energy system performance.^[1] Compared with sensible heat thermal energy storage and chemical energy storage, the latent heat thermal energy storage using phase change materials as the storage media has been an increasingly attractive technology and of interest in many engineering applications such as solar energy storage, energy-efficient building, waste heat recovery, and micro-electronic cooling.^[1] PCMs provide a high heat storage density and require a moderate operational temperature variation.^[2] The major disadvantage of phase change materials is their low thermal

conductivities which slows the rate of phase change by creating a wide internal temperature distribution.^[2] This can prolong the charging and discharging periods of a thermal management system and potentially limits the useful power that can be extracted from the energy storage medium.^[1,2]

In order to increase the rate of heat transfer within PCMs, and, therefore, improve phase change time, several enhancement techniques have been studied, such as: micro-encapsulation of PCM using graphite,^[3] silicon carbide,^[4] and nickel film coating;^[5] dispersion of high conductivity/low-density materials such as carbon fibres and metal particles;^[5] and the impregnation of PCM into high conductivity porous materials, example, porous metal (copper, aluminium or nickel) or graphite.^[6] Encapsulation of PCM gives some advantages such as reduced potential for reaction between the PCM and the container material and the ability to withstand volume change during phase change.^[7] However, its usage is limited by cost, small specific surface area of the encapsulated PCMs and the increased risk of super-cooling.^[6]

Dispersion of high conductivity particles into PCM is a relatively simple technique to enhance the thermal conductivity of PCMs. Studies involving the dispersion of high conductivity particles like copper, silver and aluminium have been undertaken in research

works reported in.^[8,9] The investigations showed that particulate fillers with high thermal conductivity and high aspect ratio are desirable for enhancing the thermal conductivity of a PCM. The major drawback of this technique is the tendency of the particles to segregate- resulting in non- uniform distribution of heat.^[9] The use of carbon fibre as a thermal conductivity enhancer for PCMs shows good promise due their low density (2260 Kg/m³), high thermal conductivity of carbon fibres (220 W/mK), strong resistance to corrosion and small diameters (10- 20 μm) which allow for uniform dispersion.^[10] The greatest drawback of carbon fibres is that they show complicated (directional dependent) heat flows because of anisotropic properties in the fibre/PCM composite.^[10] The use of high conductivity porous materials as a carrier for PCM constitutes an attractive alternative for improving heat transfer.^[6] The use of a porous conductive matrix has gained attention because of light weight, high specific surface area and continuous inter- connected pore structures.^[6] Porous structures can be made of copper, aluminium, nickel or graphite. The use of graphite is limited because of its anisotropy which is attributed to the alignment of the basal planes in the graphite crystal.^[11] The use of porous metals in enhancing PCM performance has recently attracted attention due to the high thermal conductivity provided by the metal struts which form continuous network that spreads the heat more rapidly throughout the phase change material.^[11] Also porous metals with useful thermal properties can be designed and processed in large quantities at low cost.^[12]

Majority of the studies on heat transfer enhancement of PCMs by porous metals have focused on high porosity porous metals with the porosity ranging between 85 to 98% and especially on the effects of the porous materials porosity and pore sizes on heat transfer enhancement of heat storage materials.^[13-20] The heat transfer process and performance of PCMs infiltrated into medium porosity (60- 70%) - porous metals is much less understood. The thermal efficiency of these relatively cheap porous materials which have structures that are uniquely different from the high porosity porous metals has not been well researched even though that the medium porosity porous metals produced from high thermal conductivity material such as aluminium can be manufactured at low cost^[12] and can in theory produce higher rates of heat transfer, thus resulting in shorter melting time than their high porosity equivalents due to the increased effective thermal diffusivity. Similarly, the PCM melting time has been found to be one of the essential design parameters in latent thermal energy storage systems and can be used to determine the geometrical parameters of a latent heat thermal energy storage unit.^[1] The aim of this study, therefore, is to evaluate the transient thermal behaviour of a phase change material infiltrated in medium porosity open- cell porous aluminium structures and to determine the structure- property- relationship between their thermal responses and pore structure.

2. Materials and Experimental procedure

2.1. Aluminium and stearic acid

Commercially pure aluminium (99.5 wt% Al) was used, with the thermo- physical properties shown in table 1.^[21] 99.5% pure

Table 1. Thermo- Physical Properties of 99.5% pure aluminium stearic acid^[21,22]

Material	Melting Pt(°C)	ΔH_f (KJ/Kg)	C_p (J/Kg.K)	(g/cc)	K(W/m.K)
Aluminium	646	338	897	2.7	237
Stearic Acid	68-72	225	2359.42	0.94	0.29

where ΔH_f , C_p , K and ρ are latent heat of fusion, specific heat capacity, thermal conductivity and density respectively

aluminium was chosen because it has a higher thermal conductivity compared with commonly used casting aluminium alloys. Stearic acid ($\geq 95\%$ FCC), with chemical formula- $[\text{CH}_3(\text{CH}_2)_{16}\text{COOH}]$ was used as the phase change material (PCM). The stearic acid was supplied by Sigma Aldrich, USA. Stearic acid is a linear chain fatty acid and has been used as a PCM in heat storage systems.^[22] Stearic acid was chosen because it has been found to exhibit many desirable characteristics such as high latent heat, negligible super-cooling, lower vapour pressure in the molten state, chemical inertness and stability, and good thermal reliability after a large number of melt/freeze cycles.^[22] It is odourless, non- toxic, and shows no phase segregation during phase change. It is commercially available at reasonable cost and has a suitable phase change temperature for solar passive heating applications.^[23] The Thermo- physical properties of stearic acid are shown in table 1.^[21,22]

2.2. Porous Al manufacturing, characterisation and porous Al/PCM composite preparation

Porous aluminium samples were manufactured by partially filling a 35 mm diameter flanged stainless steel mould (130 mm high) with sodium chloride beads, having different average sizes of 2.25 mm, 1.7 mm, 1.2 mm and 0.75 mm and varying packing densities. The different bead sizes formed the cells of the porous body while the different packing densities and applied pressure largely determined the relative density of the porous aluminium samples. The NaCl beads served as leachable templates and were made using a process described in^[24] which consists of the disintegration of a paste containing pre- gelatinized flour, NaCl and water in heated vegetable oil. The stainless steel mould was pre- heated to 600 °C, part- inserted into a vacuum chamber in which infiltration pressure ranging from 3.5 to 30 inHg (0.12- 1.02 bar) was applied to vary relative density and window size and, thereafter, cast with liquid aluminium at 800 °C. Cast samples were machined into $\varnothing 33 \times 45$ mm cylinders with 5 mm of solid metal left at the base of the samples to improve thermal contact between the sample and heat source and prevent PCM leakage. The sodium chloride salt beads were dissolved in a water bath maintained at 50 °C for 48 hours. The pore and window sizes of the resulting porous aluminium structures were measured using scanning electron microscopy and optical microscopy, in both cases combined with image analysis using image J v1.48 (NIH USA). Thirty optical images of each sample were captured from different sections and the pores and windows were measured using the image analysis software. The porous aluminium samples were weighed using an electronic balance and the densities of the porous samples were determined from the geometry of the samples and their masses. The porosities of the samples were

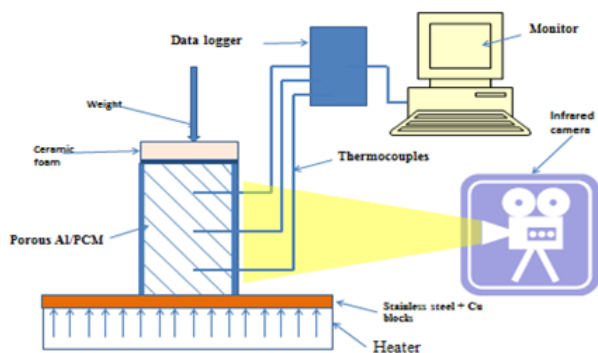


Fig. 1. Schematics of experimental set-up for thermal analysis.

determined from the calculation of their relative densities as stated in equation 1.^[25-27]

Finally PCM thermal composites were formed by inserting weighed porous aluminium samples into a beaker- packed with stearic acid blocks. The arrangement was put in vacuumed desiccator, and placed in a carbolite furnace at 80 °C. Upon melting of the PCM, the porous aluminium samples were infiltrated with stearic acid wax, cooled and re- weighed to determine the mass of PCM inside the samples.

2.3. Thermal analysis

The heat transfer characteristics of the aluminium thermal composite samples was determined by recording temperature changes with time at the sample surfaces using an infrared camera (FLIR SC7000) which was calibrated against a K- type thermocouple. PCM- filled samples were surrounded with adhesive tape (pressure sensitive tape- Scotch 2836) to prevent leakage, and sprayed with matt black paint to ensure as high emissivity as possible. An electric hot plate was used at 100 °C set- points with copper and stainless steel plates placed in between the hot plate and the sample base to serve as a heat buffer. The temperature of the samples was recorded with the infrared camera for 600 seconds. Thermographs were plotted using the maximum temperature of the infrared camera recorded at $\varnothing 4.0 \text{ mm} \pm 0.1$ around points corresponding to $\frac{1}{4}$, $\frac{1}{2}$, and $\frac{3}{4}$ of the height of the samples. The maximum temperature of the infrared camera showed the least deviation with the thermocouple readings and was

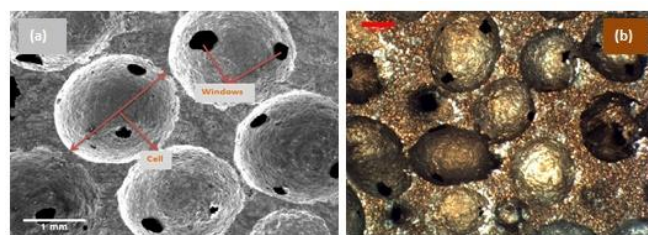


Fig. 2. (a) SEM image and (b) Optical microscope image of porous Al samples.

used. The base of the samples was coated with a silicone thermal paste (RS heat sink compound plus- RS 217-3835) to reduce contact resistance between the samples and copper block. A weight (1.2Kg) was applied at the top of the samples to improve thermal contact. Each test was run for three times. The average time for the samples to be heated from 60-80 °C was computed. The temperature range was chosen because the melting temperature of stearic acid used is 68-72 °C^[25] and it was expected that the melting of the PCM will start and end within the chosen temperature range. The experimental set-up for the thermal analysis of the aluminium thermal composite samples is shown in fig. 1. Thermal analysis of the “pure” PCM was performed using K- type thermocouples positioned at $\frac{1}{4}$, $\frac{1}{2}$, and $\frac{3}{4}$ of the height of a PCM cylinder cast into a hollow concrete (thermal conductivity, $K = 0.2\text{-}0.3 \text{ W/m.K}$ ^[26]) with inner diameter of $\varnothing 33 \times 45 \text{ mm}$ and which was mounted on an aluminium base plate with 5 mm thickness. Concrete was chosen because it has a comparable thermal conductivity with stearic acid and this will ensure one- dimensional heat flow. The PCM, encased in a hollow concrete was heated at 100 °C and temperature changes with time was recorded for 4 hours.

3. Results and Discussions

SEM and optical microscope images of empty porous aluminium structures are shown in fig. 2 while the morphological characteristics of the porous aluminium structures and degree of PCM infiltration in the porous samples are presented in Table 2. As shown in fig. 2, both SEM and optical microscope images reveal that the porous aluminium structures consist of solid matrix with spherical cells which are interconnected by “windows”. The relative density (ρ_r) of

Table 2. Morphology and degree of infiltration of aluminium thermal composite samples.

Sample	Average cell size (mm)	Average window size (mm)	Relative density	Porosity	Δm_i (g)	β
2.25/30inHg	2.25±0.09	0.40±0.03	0.38±0.02	0.62±0.02	14.92	0.75
2.25/12inHg	2.24±0.10	0.42±0.04	0.38±0.03	0.62±0.03	14.88	0.74
2.25/7inHg	2.24±0.11	0.54±0.05	0.36±0.03	0.64±0.03	14.88	0.73
2.25/5inHg	2.25±0.10	0.66±0.03	0.36±0.02	0.64±0.02	14.93	0.73
2.25/3.5inHg	2.25±0.08	0.72±0.03	0.35±0.03	0.65±0.03	14.89	0.72
1.7/30inHg	1.70±0.09	0.32±0.04	0.38±0.02	0.62±0.02	14.90	0.75
1.7/12inHg	1.71±0.10	0.39±0.03	0.37±0.03	0.63±0.03	14.96	0.74
1.7/7inHg	1.70±0.10	0.49±0.03	0.36±0.03	0.64±0.03	14.98	0.73
1.7/5inHg	1.70±0.09	0.53±0.04	0.36±0.02	0.64±0.02	14.89	0.73
1.7/3.5inHg	1.71±0.08	0.68±0.03	0.35±0.03	0.65±0.03	14.89	0.72
1.2/30inHg	1.20±0.07	0.28±0.03	0.38±0.03	0.62±0.03	14.96	0.75
1.2/12inHg	1.21±0.08	0.34±0.04	0.38±0.02	0.62±0.02	14.92	0.75
1.2/7inHg	1.20±0.09	0.40±0.03	0.36±0.03	0.64±0.03	14.90	0.73
0.75/30inHg	0.75±0.06	0.22±0.04	0.40±0.02	0.60±0.02	14.90	0.77
0.75/12inHg	0.75±0.08	0.29±0.04	0.39±0.03	0.61±0.03	14.89	0.76

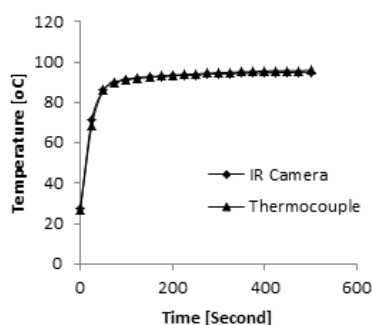


Fig. 3. Comparison between thermographs of infrared camera and K-type thermocouple at $\frac{3}{4}$ height of porous sample.

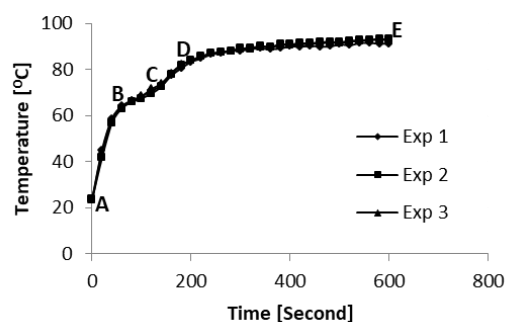


Fig. 5 Temperature versus time curves of PCM- filled porous Al samples for repeated tests.

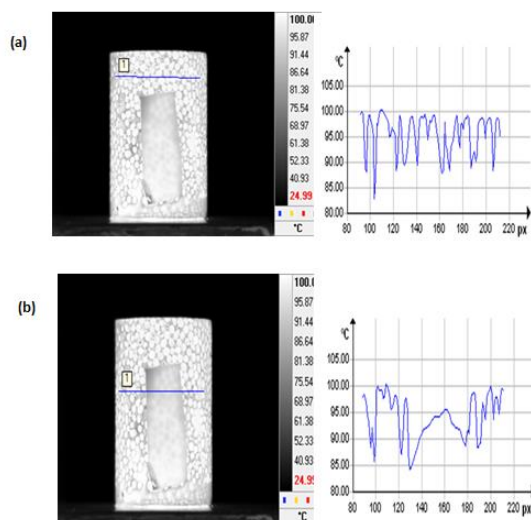


Fig. 4. Infrared camera temperature profile for empty porous sample: (a) without adhesive tape; and (b) with adhesive tape.

Fig. 4 (a) shows temperature fluctuation between a minimum and maximum value across a porous sample due to the pores in the sample while fig. 4 (b) shows the effect of adhesive tape on the surface temperature of the sample. As seen from fig. 4 (a), the temperature of the porous sample fluctuates between approximately 88 and 98 °C across a distance within the porous material. The fluctuation is probably due to the fact that the material is hottest at the struts and has the least temperature at the centre of the pores. It can be noticed from fig. 4 (b) that sticking an adhesive tape on the porous material lowered its surface temperature from a maximum of 98 to 95 °C and also reduced the minimum the minimum temperature from 88 to 86 °C resulting in a temperature drop of approximately 3 °C. However, the temperature reduction due to sticking of tapes is the same in all the samples.

Heat transfer performance of the PCM- filled porous aluminium samples can be related to the time taken by the samples to attain higher temperatures which in turn is a function of the materials effective thermal diffusivity. Heat transfer performance of the PCM- filled porous aluminium samples was evaluated by thermographic studies and by determining the average time taken by the samples to attain the temperatures of 60 °C and 80 °C and computing the amount of time Δt taken (and also Δt of one gramme of PCM) to heat the PCM through this temperature range ($t_{80} - t_{60}$). Table 3 shows the average time taken for the PCM- filled porous aluminium samples to attain the temperatures of 60 and 80 °C and the amount of time for the samples to be heated through this temperature range. As seen, Δt and $\Delta t/g$ are influenced by the relative density and window diameter of the samples. For instance, at constant window diameter of 0.40 mm, $\Delta t/g$ reduces from 8.40 seconds to 7.03 seconds as the relative density of the porous samples is increased from 0.36 for the 1.2/7inHg porous sample to 0.38 for the 2.25/30inHg giving 16.3% reduction in time. Similarly, at constant relative density of 0.38, $\Delta t/g$ decreases as the window size of the porous materials is increased from 0.28 mm for the 1.2/30inHg sample to 0.42 mm for the 2.25/16inHg sample.

Fig. 5 shows the thermographs of PCM- filled open- cell porous aluminium sample at $\frac{3}{4}$ of the height of a sample for three different tests. It can be seen that the graphs are close to each other which is an indication that thermal analysis of PCM- filled porous aluminium samples using the infrared camera is reproducible. As shown in fig. 5, the thermograph of a PCM- filled porous aluminium structure can be divided into three distinct regions: These are the solid region, AB, characterised by a steep slope in which temperature increases

the porous aluminium structures, and the degree of PCM infiltration (β) into the porous materials were respectively determined using equations 1 and 2.^[27]

$$\rho_r = \frac{\rho^*}{\rho_s} \quad (1)$$

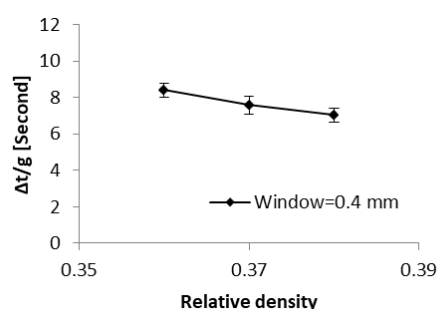
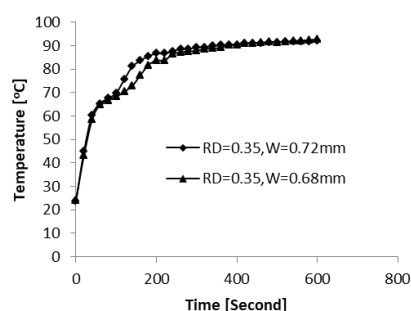
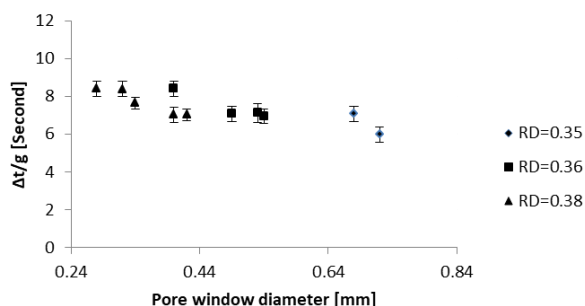
$$\beta = \frac{M_{actual}}{M_{ideal}} = \frac{\Delta m_i}{\rho_{pcm} V_t} \quad (2)$$

where ρ^* is the density of the porous material, ρ_s is the density of the solid metal, ρ_{pcm} is the density of phase change material, M is mass of PCM, Δm_i is the actual mass of PCM infiltrated in the porous aluminium structure and V_t is the total volume of porous sample. Porosity is equal to $(1 - \rho_r)$. As seen in Table 2, the relative density of the porous aluminium samples ranges between 0.35 and 0.40, the degree of infiltration of PCM in the porous samples ranges from 72 and 77% and the window diameter of the samples is between 0.22 mm and 0.72 mm. Window sizes are controlled by the bead sizes, infiltration pressure and the wetting characteristics of the molten metal- in contact with the sodium chloride beads.^[25]

Fig. 3 shows a comparison between the thermographs of empty porous aluminium sample obtained by using an infrared camera and K- type thermocouple. As seen, temperature measurement from the infrared camera compares favourably well with the K- type thermocouple readings.

Table 3: Time for PCM- filled porous Al samples to attain 60 and 80 °C at ¼ Height.

	2.25 30 inHg	2.25 16 inHg	2.25 7 inHg	2.25 5 inHg	2.25 3.5 inHg	1.7 30 inHg	1.7 12 inHg	1.7 7 inHg
t60 (sec)	42.1	44.3	41.6	38.1	40.9	43.6	47.4	50.5
t80 (sec)	147.0	148.7	145.0	127.7	130.0	157.5	161.0	157.2
Δt (sec)	104.9±0.8	104.4±0.5	101.4±0.6	89.6±0.5	89.1±0.6	113.9±0.3	113.6±0.2	106.7±0.2
Win \varnothing	0.40	0.42	0.54	0.66	0.72	0.32	0.40	0.49
ρr	0.38	0.38	0.36	0.36	0.35	0.38	0.37	0.36
PCM (g)	14.92	14.88	14.88	14.93	14.89	14.90	14.96	14.98
$\Delta t/g$	7.03	7.02	6.94	6.00	5.98	7.64	7.59	7.12
	1.7 5 inHg	1.7 3.5 inHg	1.2 30 inHg	1.2 12 inHg	1.2 7 inHg	0.75 30 inHg	0.75 12 inHg	
t60 (sec)	47.3	46.4	46.1	51.6	46.6	85.5	86.3	
t80 (sec)	152.8	151.6	171.6	177.0	171.8	231.9	230.8	
Δt (sec)	105.5±0.4	105.2±0.2	125.5±0.2	125.4±0.4	125.2±0.3	146.4±0.7	144.5±0.4	
Win \varnothing	0.53	0.68	0.28	0.34	0.40	0.22	0.29	
ρr	0.36	0.35	0.38	0.38	0.36	0.40	0.39	
PCM (g)	14.89	14.87	14.96	14.92	14.90	14.90	14.89	
$\Delta t/g$	7.08	7.07	8.39	8.40	8.40	9.83	9.70	

**Fig. 6.** Effect of relative density on the time for PCM- filled porous aluminium samples heated from 60 to 80 °C at constant pore diameter.**Fig. 8.** Effect of pore window size on the variation of temperature with time for stearic acid PCM infiltrated in porous Al samples with constant relative density.**Fig. 7.** Effect of pore window size on the time for PCM- filled porous aluminium samples heated from 60 to 80 °C at constant relative density.

linearly with time; the melting (mushy) region, BC, in which the temperature rise with time is nearly constant and at which melting is completed; and a molten region, CDE, which is characterised by a steep gradient and a near steady state region in which the temperature of the PCM approaches that of the heat source.

3.1. Effect of relative density on heat transfer performance of PCM thermal composites

The effect of relative density on the time for the heating of PCM-filled open-cell porous aluminium samples having the same window size through 60- 80 °C (Δt) is shown in fig. 6. It can be seen that Δt decreases as the relative density of the porous aluminium samples is increased from 0.36 to 0.38. The increase in heat transfer

performance is probably because, as the relative density of the thermal composite samples is increased, the volume fraction of their metal constituents increases. The increased metal fraction increases the effective thermal conductivity and hence the thermal diffusivity of the PCM thermal composites and this ultimately increases heat transfer by conduction.

3.2. Effect of window size on heat transfer performance of PCM thermal composites

The effect of window diameter on the time for the PCM- filled porous aluminium samples to be heated from 60 to 80 °C is shown in fig. 7 while the thermographs of stearic acid PCM infiltrated in porous aluminium structures having the same relative density and varying window sizes are shown in fig. 8. As shown in fig. 7, at constant relative density, Δt decreases as the window diameter of the porous aluminium samples is increased while as can be seen in fig. 8, the sample with larger window ($\rho r=0.35, W=0.72\text{mm}$) showed faster temperature rise with time and melting process than the sample with smaller window size. It can be deduced from these figures that the heat transfer performance of the stearic acid PCM, increases as the window diameter of the open-cell porous aluminium structures is increased. The reason is probably because although the porous aluminium samples with smaller pore window sizes can enhance heat transfer by providing larger heat transfer surfaces, as melting progresses and the liquid PCM phase increases in size, natural convection tends to play a significant role due to buoyancy effect

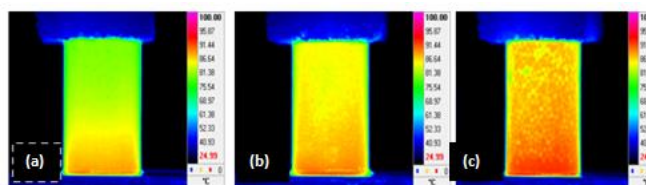


Fig. 9. Picture representation of temperature changes with time for: (a) 0.75/12inHg; (b) 1.7/30inHg; and (c) 2.25/3.5inHg samples heated at 100 °C for 300 seconds.

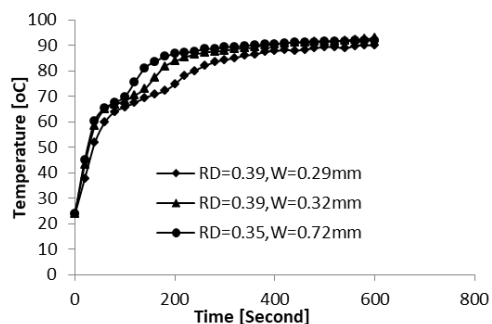


Fig. 10. Comparison between thermographs of the 0.75/12inHg, 1.7/30inHg and 2.25/3.5inHg samples

generated by density difference between the solid and liquid phases of the PCM. The natural convection flow of liquid PCM is also strengthened by the effect of pressure gradient due to volume change from solid to liquid which makes the molten PCM to flow upwards. Smaller window size would lead to lower permeability and more suppression of natural convection and motion of liquid PCM and hence the weakening of the overall heat transfer and melting process.^[16]

3.3. Comparison between heat transfer performance of PCM/porous aluminium composite structures and pure stearic acid

Fig. 9 shows picture presentation of temperature changes within the 2.25/3.5inHg; 1.7/30inHg and 0.75/12inHg samples, heated at 100 °C for 300 seconds. The samples have different relative density and window sizes and were selected to represent samples with relatively high, medium and low heat transfer performance. The increase in temperature of the samples as indicated by the changes in colour of the infrared camera images for the respective samples is in the following order: 0.75/12inHg < 1.7/30inHg < 2.25/3.5inHg. This trend of behaviour is also shown in fig. 10 in which the 2.25/3.5inHg sample showed the fastest heat transfer rate and the shortest melting time and was followed by the 1.7/30inHg sample and then the 0.75/12inHg sample. The 0.75/12inHg sample despite having the highest relative density and least window size showed the least heat transfer performance. This is probably because the high relative density and small window size of the 0.75/12inHg sample resulted in its low permeability and which in turn gave rise to the dampening of the convection motion of the liquid PCM which naturally enhances convection heat transfer.^[28] This suggests that ultimate heat transfer performance of PCM thermal composites is a balance between contributions from heat conduction through the porous metallic struts which expectedly increases with relative density and the ability of the samples to allow for contributions from natural convection

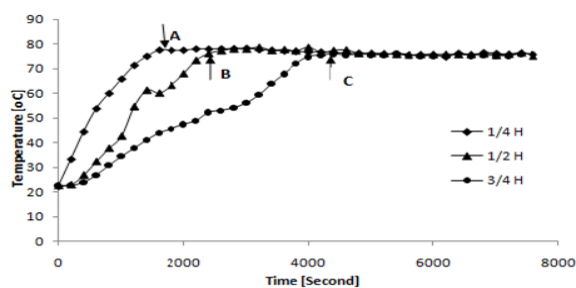


Fig. 11. Temperature Vs time curves for pure stearic acid PCM heated at 100 °C

Table 4: Time for pure stearic acid and PCM- filled porous Al samples to attain 70 °C.

Sample	Amount of PCM (g)	Time to attain 70 °C (second)	Time to attain 70 °C (second)
2.25/3.5inHg	14.89	97.9	6.57
1.7/30inHg	14.90	117.5	7.89
0.75/12inHg	14.89	160.4	10.77
Pure PCM	42.45	3675	86.57

through offering lesser resistance to convective motion of liquid PCM by possessing optimally wide windows.

Points A, B, and C in fig. 11 are the estimated points for the commencement of melting at the $\frac{1}{4}$, $\frac{1}{2}$ and $\frac{3}{4}$ of the height of the pure stearic acid sample. Melting is estimated to occur between 72-74 °C. This is slightly out of the range of the melting temperature range for the $\geq 95\%$ FCC stearic acid used as phase change material. The discrepancy may be due to the differential heating rates for the DSC analysis and experimental samples.^[29]

The times for the pure stearic acid PCM and for the stearic acid infiltrated in 2.25/3.5inHg, 1.7/30inHg, 0.75/12inHg samples to attain the temperature of 70 °C at $\frac{3}{4}$ of the height of the samples are presented in Table 4.

Table 4 suggests that the response time of the 2.25/3.5inHg, 1.7/30inHg and 0.75/12inHg samples are respectively 13X, 10X and 8X faster than the thermal response time of the pure stearic acid. The faster heat transfer rate of the thermal composite samples could be attributed to the higher thermal conductivity of aluminium struts (237 W/m.K^[22]) than the thermal conductivity of stearic acid (0.29 W/m.K^[23]) which results in higher effective thermal conductivity of the thermal composites. Also the aluminium struts break up the PCM into smaller cells and transfer heat by conduction to the phase change material while heat transfer in the pure stearic acid wax is slowed down by the low thermal conductivity of stearic acid and slowly occurring natural convection in the liquid state.^[20]

4. Conclusions

Experimental study was carried out to investigate the heat transfer performance of stearic acid PCM infiltrated in porous aluminium structures which were manufactured by forcing liquid aluminium through the pore spaces in loosely packed sodium chloride beads. A test rig was built to measure the rate of temperature increase in the thermal composites during a phase change process. It was observed that the morphology of the porous structure has significant effect on

the heat transfer performance of the thermal composites. By increasing porosity and window size, the melting process was accomplished faster as compared with porous aluminium structures with lower porosity and smaller window sizes. Overall heat transfer performance can be said to be a balance between relative density and window size which optimizes the heat transfer contributions from conduction and convection. It was also observed that the porous aluminium samples can give up to thirteen times improvement in heat transfer performance when compared to pure stearic acid.

Acknowledgements

The financial assistance of the Tertiary Education Trust Fund (TETFUND), Nigeria in providing funds for this research work is gratefully acknowledged.

Conflicts of Interest

The authors declare no conflict of interest.

References

- Chen Z.; Cao L.; Shan F.; Fang G. Preparation and Characteristics of Microencapsulated Stearic Acid as Composite Thermal Energy Storage Material in Buildings. *Energy Build.*, 2013, **62**, 469-474. [[CrossRef](#)]
- Sharma A.; Tyagi V.V.; Chen C.R.; Buddhi D. Review on Thermal Energy Storage with Phase Change Materials and Applications. *Renewable Sustainable Energy Rev.*, 2009, **13**, 318-345. [[CrossRef](#)]
- do Couto Aktay K.S.; Tamme R.; Müller-Steinhagen H. Thermal Conductivity of High-Temperature Multicomponent Materials with Phase Change. *Int. J. Thermophys.*, 2008, **29**, 678-692. [[CrossRef](#)]
- Pitié F.; Zhao C.Y.; Cáceres G. Thermo-mechanical analysis of ceramic encapsulated phase-change-material (PCM) particles. *Energy Environ. Sci.*, 2011, **4**, 2117-2124. [[CrossRef](#)]
- Maruoka N.; Akiyama T. Thermal Stress Analysis of PCM Encapsulation for Heat Recovery of High Temperature Waste Heat. *J. chem. Eng. Jpn.*, 2003, **36**, 794-798. [[CrossRef](#)]
- Fernandes D.; Pitié F.; Cáceres G.; Baeyens J. Thermal Energy Storage: "How Previous Findings Determine Current Research Priorities". *Energy*, 2012, **39**, 246-257. [[CrossRef](#)]
- Hawladar M.N.A.; Uddin M.S.; Khin M.M. Microencapsulated PCM Thermal-Energy Storage System. *Appl. Energy*, 2003, **74**, 195-202. [[CrossRef](#)]
- Khodadadi J.M.; Hosseinzadeh S.F. Nanoparticle-Enhanced Phase Change Materials (NEPCM) with Great Potential for Improved Thermal Energy Storage. *Int. Commun. Heat Mass Transfer*, 2007, **34**, 534-543. [[CrossRef](#)]
- Oya T.; Nomura T.; Tsubota M.; Okinaka N.; Akiyama T. Thermal Conductivity Enhancement of Erythritol as PCM by Using Graphite and Nickel Particles. *Appl. Therm. Eng.*, 2013, **61**, 825-828. [[CrossRef](#)]
- Zhao Y. Porous Metallic Materials Produced by P/M Methods. *J. Powder Metall. Min.*, 2013, **2**, e113. [[CrossRef](#)]
- Han J.H.; Cho K.W.; Lee K.H.; Kim H. Porous Graphite Matrix for Chemical Heat Pumps. *Carbon*, 1998, **36**, 1801-1810. [[CrossRef](#)]
- Haowei W.; Guoding Z.; Renjie W. The Liquid Infiltration and Filling Process for Fiber Reinforced Metal Matrix Composites. *Acta Materialia Composita Sinica*, 1995, **12**, 38-42. [[Link](#)]
- Zhao C.Y.; Wu Z.G. Heat Transfer Enhancement of High Temperature Thermal Energy Storage using Metal Foams and Expanded Graphite. *Sol. Energy Mater. Sol. Cells*, 2011, **95**, 636-643. [[CrossRef](#)]
- Zhou D.; Zhao C.Y. Experimental Investigations on Heat Transfer in Phase Change Materials (Pcms) Embedded in Porous Materials. *Appl. Therm. Eng.*, 2011, **31**, 970-977. [[CrossRef](#)]
- Chintakrinda K.; Weinstein R.D.; Fleischer A.S. A Direct Comparison of Three Different Material Enhancement Methods on the Transient Thermal Response of Paraffin Phase Change Material Exposed to High Heat Fluxes. *Int. J. Therm. Sci.*, 2011, **50**, 1639-1647. [[CrossRef](#)]
- Li W.Q.; Qu Z.G.; He Y.L.; Tao W.Q. Experimental and Numerical Studies on Melting Phase Change Heat Transfer in Open-Cell Metallic Foams Filled with Paraffin. *Appl. Therm. Eng.*, 2012, **37**, 1-9. [[CrossRef](#)]
- Xiao X.; Zhang P. Morphologies and Thermal Characterization of Paraffin/Carbon Foam Composite Phase Change Material. *Sol. Energy Mater. Sol. Cells*, 2013, **117**, 451-461. [[CrossRef](#)]
- Xiao X.; Zhang P.; Li M. Preparation and Thermal Characterization of Paraffin/Metal Foam Composite Phase Change Material. *Appl. Energy*, 2013, **112**, 1357-1366. [[CrossRef](#)]
- Chen Z.; Gao D.; Shi J. Experimental and Numerical Study on Melting of Phase Change Materials in Metal Foams at Pore Scale. *Int. J. Heat Mass Transfer*, 2014, **72**, 646-655. [[CrossRef](#)]
- Mancin S.; Diani A.; Doretto L.; Hooman K.; Rossetto L. Experimental Analysis of Phase Change Phenomenon of Paraffin Waxes Embedded in Copper Foams. *Int. J. Therm. Sci.*, 2015, **90**, 79-89. [[CrossRef](#)]
- Accessed online on April 30, 2015. [[Link](#)]
- Sarı A.; Biçer A.; Karaipekli A. Synthesis, Characterization, Thermal Properties of a Series of Stearic Acid Esters as Novel Solid-Liquid Phase Change Materials. *Mater. Lett.*, **63**, 1213-1216. [[CrossRef](#)]
- Wang Y.; Xia T.D.; Feng H.X.; Zhang H. Stearic Acid/Polymethylmethacrylate Composite as Form-Stable Phase Change Materials for Latent Heat Thermal Energy Storage. *Renewable Energy*, **36**, 1814-1820. [[CrossRef](#)]
- Jinnapat A.; Kennedy A. The Manufacture and Characterisation of Aluminium Foams made by Investment Casting using Dissolvable Spherical Sodium Chloride Bead Preforms. *Metals*, 2011, **1**, 49-64. [[CrossRef](#)]
- Accessed online on June 15, 2014. [[Link](#)]
- Accessed online on September 16, 2016. [[Link](#)]
- Bai M.; Chung J.N. Analytical and Numerical Prediction of Heat Transfer and Pressure Drop in Open-Cell Metal Foams. *Int. J. Therm. Sci.*, 2011, **50**, 869-880. [[CrossRef](#)]
- Mesalhy O.; Lafdi K.; Elgafy A.; Bowman K. Numerical Study for Enhancing the Thermal Conductivity of Phase Change Material (PCM) Storage using High Thermal Conductivity Porous Matrix. *Energy Convers. Manage.*, 2005, **46**, 847-867. [[CrossRef](#)]
- Wang Y.; Xia T.D.; Zheng H.; Feng H.X. Stearic Acid/Silica Fume Composite as Form-Stable Phase Change Material for Thermal Energy Storage. *Energy Build.*, 2011, **43**, 2365-2370. [[CrossRef](#)]



© 2020, by the authors. Licensee Ariviyal Publishing, India. This article is an open access article distributed under the terms and conditions of the Creative Commons Attribution (CC BY) license (<http://creativecommons.org/licenses/by/4.0/>).